

The effect of photodynamic treatment on the morphological and mechanical properties of the HeLa cell line

Petr Kolar¹, Katerina Tomankova¹, Jakub Malohlava¹, Jana Zapletalova¹, Milan Vujtek², Klara Safarova³, Dalibor Jancik^{2,3} and Hana Kolarova¹

¹ *Department of Medical Biophysics, Faculty of Medicine and Dentistry, Institute of Molecular and Translational Medicine, Palacky University, Hnevotinska 3, 775 15 Olomouc, Czech Republic*

² *Department of Experimental Physics, Faculty of Science, Palacky University, 17. Listopadu 12, 771 46 Olomouc, Czech Republic*

³ *Regional Centre of Advanced Technologies and Materials, Faculty of Science, Palacky University, 17. Listopadu 12, 771 46 Olomouc, Czech Republic*

Abstract. High resolution imaging of biological structures and changes induced by various agents such as drugs and toxins is commonly performed by fluorescence and electron microscopy (EM). Although high-resolution imaging is possible with EM, the requirements for fixation and staining of samples for image contrast severely limits the study of living organisms. Atomic force microscopy (AFM), on the other hand, is capable of simultaneous nanometer spatial resolution and piconewton force detection, allowing detailed study of cell surface morphology and monitoring cytomechanical information. We present a method that images and studies mechanically characterized cells using AFM. We used a HeLa cell line (cervix carcinoma cell), which is sensitive to photodynamic treatment (PDT); growth media as a scanning surrounding; atomic force microscopy NT-MDT Aura for cytomechanical measurement; and scanning electron microscope Hitachi Su 6600 for control images of the cells. The modulus of elasticity for intact and photodynamically damaged cells can indicate mechanical changes to the main properties of cells. Cell elasticity changes can provide information on the degree or value of cell damage, for example after PDT. Measurements were carried out on approximately sixty cells, including three independent experiments on a control group and on sixty cells in a photodamaged group. Cells before PDT show higher elasticity: the median of Young's modulus on the nucleus was 35.283 kPa and outside of the nucleus 107.442 kPa. After PDT, the median of Young's modulus on the nucleus was 61.144 kPa and outside of the nucleus was 193.605 kPa.

Key words: Atomic force microscopy — Photodynamic treatment — Cytomechanical properties — Young's modulus

Introduction

Cell lines can be studied using various microscopic techniques such as fluorescence, confocal, scanning electron microscopy (SEM) or transmission electron microscopy (TEM). These methods deliver the best resolution. How-

ever, some of them (at least TEM or SEM), require extensive sample preparation, including thorough fixation procedure and drying, to avoid inhomogeneous sample shrinkage (Jung et al. 2009). Despite enormous advances in cancer biology, there is an increased demand for new technologies. The past decade has witnessed the emergence of atomic force microscopy (AFM) from solid-state physics into cell biology and even medicine (Sullivan et al. 2007). AFM is a technique for imaging biological samples at subnanometer resolution (Casuso et al. 2011). This technique not only records the surface topography of biological samples under physiological conditions (Haga et al. 2000), it also

Correspondence to: Katerina Tomankova, Department of Medical Biophysics, Faculty of Medicine and Dentistry, Institute of Molecular and Translational Medicine, Palacky University, Hnevotinska 3, 775 15 Olomouc, Czech Republic
E-mail: katerina.tomankova@upol.cz

permits study of micromechanical properties of the living cells (Riethmuller et al. 2007; Vegh et al. 2012), binding constants and electrical or magnetic characteristic at high spatial resolution and force sensitivity (Kuznetsova et al. 2007; Sugitate et al. 2009). Force scanning in particular can be used for mapping the mechanical properties of adherent living cells and provides information on cellular structures, including the cytoskeleton (Leporatti et al. 2009) with low demands on sample preparation (Mustata et al. 2010). The elasticity of a cell provides important information on the health and function of the cell, and this information can be obtained using the AFM *via* force curve measurements over an extended area (sometimes referred to as force volume).

Eukaryotic cells generally contain three distinct types of polymer biomolecules that serve as structural elements in the cytoskeleton of the cell: actin microfilaments, vimentin intermediate filaments, and microtubules (tubulin). F-actin provides the highest resistance to deformation up to a certain critical value of local strain. Intermediate filaments are sufficiently compliant to generate moderate deformation, and yet maintain their resistance to shear deformation under large local strains to provide the structural integrity to the cell. Microtubules do not have sufficient tensile or shear stiffness to impart significant mechanical integrity to the cytoskeleton. However, they act in concert with the other filamental biopolymers to stabilize the cytoskeleton (Suresh 2007). Disturbance in these systems have been related to tumor progression and metastasis (Casas et al. 2008).

Different studies demonstrated the correlation of the mechanical properties of the cells (stiffness, elasticity) with several processes including cell growth, cell death, adhesion differentiation, migration, carcinogenesis, effect of oxidative stress and attack of viruses or parasites (Mustata et al. 2010). Vileno and co-workers observed that oxidative stress-induced changes were larger in the actin-rich region (lamellipodium) than in the cell body (Vileno et al. 2004). It is known that differences in the Young's modulus between normal and cancerous human epithelial cells were found to be due to a different organization of the cell cytoskeleton (Li et al. 2008) and this was the case with normal and cancerous human cervical epithelial cells (Muller and Dufrêne 2011). For example, breast carcinoma cells, MCF7, behave as a complex linear viscoelastic material in the applied load range (0.5–4 nN) (Moreno-Flores et al. 2010); metastatic or cancer cells from the patients are softer than healthy cells. Young's modulus of normal ovarian mouse cells CHO-K1 is 1.02 kPa in comparison with cancerous cells of the same cell line – 0.244 kPa, or human mesothelial (CF) cells – a normal cell has 1.97 kPa while a cancerous one has 0.53 kPa (Ketene et al. 2012). Human bronchial epithelial cells showed an increase in cytoskeleton stiffness during metastasis (Leporattiet al. 2009). Moreover, the nuclear

portion is softer (4 kPa) than other parts of NIH3T3 living cells except for a small area in the perinuclear region (Haga et al. 2000).

Photodynamic treatment (PDT) is a promising anti-cancer therapy that uses photosensitizers, often porphyrin or phthalocyanine derivatives, with a selective affinity to cancer cells and photooxidation activity following adsorption of visible light of a specific wavelength (Kolarova et al. 2008). PDT offers several advantages over the conventional cancer treatments, such as a minimal systemic toxicity, high selectivity to the tumor, few secondary effects, the possibility of repetitive cycles of treatments and the combination with other therapies, for example chemo and radiotherapy (Sanabria et al. 2013).

Phthalocyanines belong to the new generation of sensitizers and can be chelated with metals (i.e. aluminium and zinc) to enhance their phototoxicity. A ring substitution in phthalocyanines with sulphonated groups allowed better hydrophilicity of photosensitizer ClAlPcS₂. The distribution of aluminium phthalocyanine (AlPc) is diffused through the cytoplasm. Disulfonated and tetra-sulfonated aluminium phthalocyanine (AlPcS₂, AlPcS₄) are localized in vesicles suggestive of lysosomes (Malham et al. 1996). Photosensitization of target cells or tissues with light of an appropriate wavelength causes a cascade of biological events through various photophysical pathways which induce reactive oxygen species (ROS), mitochondrial membrane depolarization, elevation of intracellular Ca²⁺, activation of caspases and ultimately result in cell death through apoptosis or necrosis. PDT induces changes in cytoskeletal components such as microtubules and microfilaments and changes in cell elasticity (Uzdensky et al. 2005; Jung et al. 2009). Fernández-Guarino reveal mitochondrial dysfunction, along with increased cell adhesion and reorganization of components of the cytoskeleton during photodynamic therapy (Fernández-Guarino et al. 2007). Aminolevulinic acid (ALA) PDT-induced increase of the number of stress fibres in WiDr cells may indicate a strengthening of the cell-substratum contact. Changes in cell adhesion are accompanied with the remodelling of the actin cytoskeleton (Uzdensky et al. 2005). ALA-mediated disruption of filamental actin structure (actin filaments formed clusters and the plasma membrane lost its ring-like structure) and alteration in the phosphorylation/expression of cytoskeletal protein septin-2 and cofilin within three hours after completing the treatment (Pluskalova et al. 2006).

This study focuses on cytomechanical (elasticity) measurements of adherent cervix cancer cells under physiologically relevant conditions and after photodynamic treatment. The mechanics of cancer cell deformability and its interactions with the extracellular physical, chemical, and biological environments offer enormous potential for significant new developments in disease diagnostics, thera-

peutics and drug efficacy assays (Li et al. 2008). Our study focuses on biomechanics and the biophysical properties of cells and it is important in the understanding of the onset and progression of disease states, for example cancer at the cellular level. Our study demonstrates the importance of the combined use of traditional and relatively novel microscopy techniques during cell death caused by PDT. The biomechanical characterization can be an important step for a deeper understanding of cervical cancer. It is expected that the approaches described in this paper for studying cells by AFM will also be relevant to investigations of other cancer cell types and this study will open a new way of evaluating cell damage after photoinduction.

Materials and Methods

Material and instruments

In our experiments, we used the HeLa cell line (Virus epithelioid cervix carcinoma) as a biological material. We used Thermanox® sterile plastic microscope slides as substrates for cells (Nunc) and 35 mm Petri dishes (Iwaki) for cultivation of the cell line. Chemicals used were Dulbecco's Modified Eagle Medium (DMEM) with 10% fetal bovine serum (FBS, Sigma) and 2% 200 mM L-glutamine and 0.4% penicillin/streptomycin (Sigma), sensitizer ClAlPcS₂ (prepared by Jan Rakusan at the Research Institute for Organic Syntheses in Rybitvi, Czech Republic), glutaraldehyde (GA, Sigma). Measurements were carried out on AFM Ntegra Aura (NT-MDT), AFM Bioscope Catalyst (Veeco), NSG10 tip (NT-MDT), CSG10 tip (NT-MDT), transmission microscope Olympus IX81 with DSU unit (Olympus), SEM Hitachi Su6600 (Hitachi).

Cell culture

2×10^5 HeLa cells were cultivated in a DMEM medium under a humidified 5% CO₂-atmosphere on plastic cover slips coated with poly-L-lysine (PLL, 0.01%, incubation 24 h at room temperature, twice washed with distilled water) for 24 h at 37°C. After incubation, cells for imaging were gently fixated by 0.5% glutaraldehyde directly added into the medium for 20 min at 37°C and 5% CO₂. Cells were scanned in fresh DMEM (for AFM) or dry (for SEM imaging) at room temperature. Mechanical mapping was done on non-fixed living cells.

Photodynamic treatment

2×10^5 HeLa cells were placed in 35 mm Petri dishes with Thermanox plastic discs and 2 ml cultivation medium DMEM. Photosensitizer ClAlPcS₂ was added in concentra-

tions of 0 (control) and 5 μM. After 24 h incubation at 37°C and 5% CO₂ dishes with the sensitizer, the cells were irradiated with a dose of 15 J/cm². For the irradiation, we used light emitting diodes (LED) with the emission wavelength maximum at 660 nm, FWHM 25 nm. The light intensity used was 10 mW/cm² for 25 min up to a dose of 15 J/cm² using an LED irradiator. After this treatment, cells were cultivated for the next 6 h under the same conditions in a fresh DMEM medium.

SEM imaging

Cells were measured in the regime of secondary electron (SE) with accelerating voltage of 0.5 and 1 kV and magnification \times (1500–6000). Cells were applied to Thermanox discs on a titanium holder.

AFM imaging

Cells were imaged with a scan rate of 0.3–0.6 Hz. We used a NSG10 tip with a resonant frequency of 190–325 kHz and a force constant of 5.5–22.5 N/m for imaging and a CSG10 tip with a resonant frequency of 8–39 kHz and a force constant of 0.01–0.5 N/m for living cell mechanical mapping (AFM Bioscope Catalyst). AFM surface images were acquired in a semi-contact topography mode (AFM Ntegra Aura). All images were processed by Nova software (NT-MDT) and force curves were analyzed by the force curve analysis module of SPIP (Image Metrology).

Elasticity measuring

The area was scanned at higher resolution and a single isolated cell of interest was identified within the scanned area. After recording this scan, the cursor was placed on the identified cell and force curves were measured. Approximately twenty cells were measured in each of the three independent experiments of the control group and the photo-damaged group. A subsequent image was generated to confirm that the condition and location of the cell of interest had not been changed by the force curve measurements. For our samples, we used Sneddon's generalization of the Hertz model of contact (Sneddon 1965), as implemented in SPIP. In this model, the loading force F , exerted by the tip, causes a deformation of the sample, δ . With the assumption of an infinitely hard tip (appropriate for cell investigation), conic tip shape and non-adhesive interaction, Sneddon's model gives the following relation between force and cell deformation:

$$F = \frac{2}{\pi} \frac{E}{1 - \nu^2} \tan(\alpha) \delta^2$$

where α is the tip half cone angle, E is the measured Young's modulus and ν is the Poisson's ratio of a cell, and δ is the cell deformation. Several complications are related to the previous equation. Determination of Young's modulus was performed by fitting the above-mentioned equation. Baseline correction was performed by SPIP from the approach curve and the point of zero indentation was determined automatically. Cantilever sensitivity was obtained from measurement on a hard sapphire plate. Poisson number was set to 0.5.

Cantilever spring constant determination

For Young's modulus measurement, the cantilever spring constant k must be known. We used the modified Sader method, provided by a Nova software script. This method is based on the measurement of unloaded resonance frequency of the cantilever, ω_0 , and the spring constant is computed from this frequency and from geometrical dimensions. The modified Sader method (Sader 1999), valid for rectangular cantilevers, uses an imaginary component of hydrodynamic function Γ_i , thus taking into account the viscous damping of ambient air. The final equation can be written in the form $k = 0.1906\rho b^2 l Q \Gamma_i(\omega_0) \omega_0^2$, where ω_0 and the quality factor Q are determined from the resonance curve by the script; cantilever width b and length l are taken from the cantilever manufacturer's specifications and air density ρ and viscosity are tabular values at actual room temperature.

Statistical analysis

The results were processed using software SPSS v. 15 (SPSS Inc. Chicago, USA). The data are presented as median, quartil²⁵ and quartil⁷⁵, of three independent experiments in four groups (C, C-Nucleus and PDT, PDT-Nucleus). The PDT groups were compared with control groups using the Mann-Whitney U-test. The statistical analysis of the results of Young's modulus in defined intervals was performed using Fisher exact tests. The value $p < 0.05$ was considered statistically significant.

Results and Discussion

The determination of the local elastic properties of cells under cultured conditions enables us to measure the influence of various factors on the mechanical properties of living cells. AFM measurement of the mechanical properties of cells appears to be promising in the diagnostics of different pathologies (Nikkhah et al. 2010). When studying the mechanical properties of a cell by AFM methods, we deal predominantly with the heterogeneity of the plasma mem-

brane (lipid domains, protein complexes) (Starodubtsteva 2011). The results are presented to illustrate how changes in the cell cytoskeleton, induced by cancer treatment, can significantly influence cell mechanics.

PDT induced dramatic changes in cell morphology and the cytoskeleton, depending on the light dose, concentration of the sensitizer and post-irradiation time (Tomankova et al. 2007; Casas et al. 2008; Jung et al. 2009). At 10 s, PDT induced a slight cell shrinkage and the initiation of microtubule disruption, with no significant change to the microfilaments. In addition, small vesicles began to appear in the cell membrane (Jung et al. 2009). After PDT, some cells retracted their lamellipodia and formed extracellular blebs containing tubulin. In HeLa cells, the microtubular cytoskeleton was disaggregated so that the tubulin was concentrated in the perinuclear region. Necrotic blebbing was observed 30 minutes after irradiation (Uzdensky et al. 2005). On the other hand, after PDT was observed, there was an emission of filopodia and extensive surface blebbing again in HeLa cells. These morphological changes were paralleled by the rearrangement of the cytoskeletal components: tubulin network were reorganized into thick bundles that at longer recovery times were concentrated inside the blebs. In parallel with the observed changes in cell shape, actin microfilaments formed bundles, especially at the cell periphery, which became progressively thicker with increasing post-irradiation times. Apoptotic blebbing was observed with a longer irradiation time (Panzarini et al. 2006).

At 300 s, PDT induced apparent cell shrinkage with a growth of membrane vesicles and profound disruption of microtubules. Extreme cell shrinkage and microtubule disruption were observed at 600 s after PDT, and disrupted microtubules were evident as massive membrane and extracellular vesicles. Interestingly, membrane microtubule vesicles were surrounded by reorganized microfilaments, whereas extracellular elongated microtubule vesicles were localized on extracellular microfilaments. More extreme changes in cell morphology and the cytoskeleton were observed at 10 min after PDT, when massive growth of the membrane blebs and the disruption in the cytoskeleton were observed (Jung et al. 2009). For these reasons, PDT provides a good method for investigating changes within the cytoskeleton ultrastructure. In our case, after treatment we waited about 6 hours for apoptosis/necrosis expression.

Morphological classification has been described by the SEM (Figure 1) and AFM technique (Figure 2 and 3). The cells appear quite flat as a result of the drying procedure, with the prominent nucleus in the centre surrounded by its nuclear envelope. The height of untreated cells shown in Figure 2 was 1.33 μm , 40.18 μm long and 18.06 μm wide. To obtain information about the cell morphology, AFM

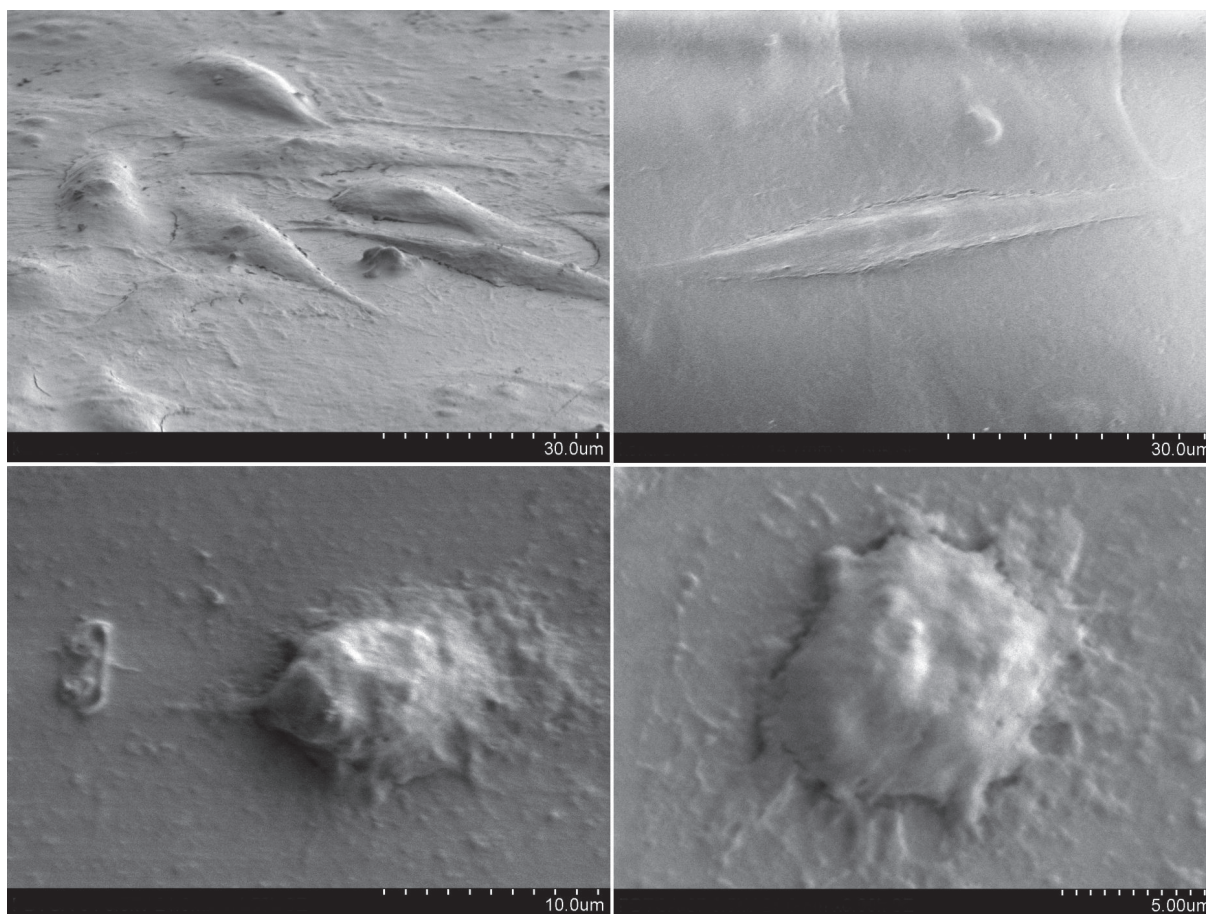


Figure 1. Scanning electron imaging of HeLa cell line fixated by 0.5% glutaraldehyde on the Thermanox coverslip before (top) and after photodynamic treatment (bottom, CIAIPcS₂ was added in concentrations 5 μM and irradiated with dose of 15 J/cm²). Thermanox coverslips were applied onto a titanium holder. Cells were measured in the regime of secondary electron with accelerating voltage of 0.5 and 1 kV and magnification × 1500–6000.

observations were complemented with force measurement observations. Cells before PDT have tendency to form dense colonies, resulting in difficulties for force imaging at the cellular level and in probing lateral domains involved in cell-cell interaction (Leporatti et al. 2009). On the other hand, cells after treatment grew independently of other cells. Cells after photodynamic treatment (Figure 3) had a different size in relation to untreated cells: 1.78 μm in height, 21.06 μm in length, and 20.8 μm in width. SEM can easily localize intracellular biomolecules in 2- or 3-dimension, but cannot resolve structures at the molecular level, whereas AFM can provide ultrastructural information at the molecular level, but is limited to analysis of surface topography. Probing of the cell surface by AFM techniques can reveal heterogeneities of mechanical properties of the surface at the nanolevel, and subsurface layers of cells. The resolution of AFM in air in the vertical direction is 0.1–0.5 nm, and 1–5 nm in the horizontal direction, depending on the sample rigidity. The

horizontal resolution can be solved for living cells in aqueous medium even at several tens of nanometer range due to the softness of the cell membrane. The thickness of cellular membranes is known to be around 5–10 nm. The sensitivity and resolution of the AFM method also depend on tip and cantilever characteristics (e.g., radius, shape, material) (Kuznetsova et al. 2007).

The imaging of cell lines requires that the cells are stably immobilized, so that they are not displaced by forces generated by the tip during scanning. For this reason we used poly-L-lysine for better adhesion to substrate. However, no significant effect to cell elasticity was observed. Immobilization procedures are established for cell lines and have facilitated investigations on elasticity, adhesion, surface structure, and swarming behavior (Sullivan et al. 2007). After cross-linking the cellular proteins with the fixative glutaraldehyde, plasma membrane depressions become observable and are scattered around the cell nucleus. It

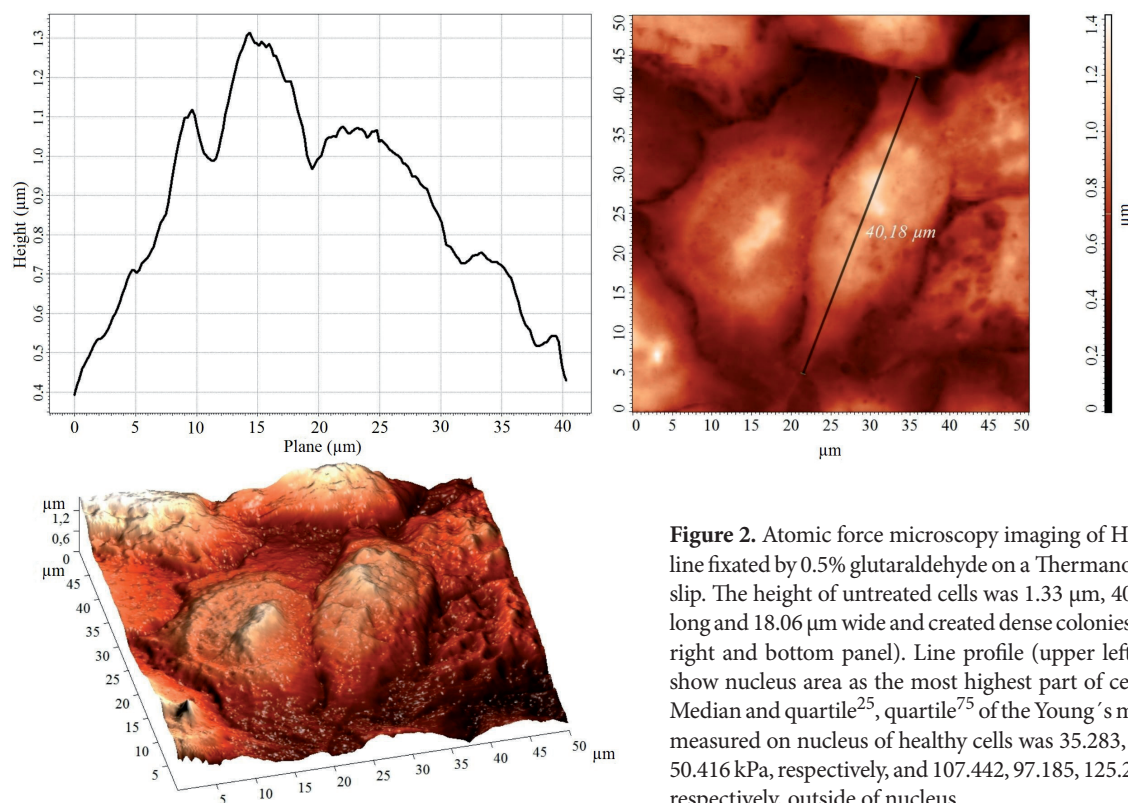


Figure 2. Atomic force microscopy imaging of HeLa cell line fixated by 0.5% glutaraldehyde on a Thermanox cover slip. The height of untreated cells was 1.33 μm , 40.18 μm long and 18.06 μm wide and created dense colonies (upper right and bottom panel). Line profile (upper left panel) show nucleus area as the most highest part of cell body. Median and quartile²⁵, quartile⁷⁵ of the Young's modulus measured on nucleus of healthy cells was 35.283, 28.061, 50.416 kPa, respectively, and 107.442, 97.185, 125.270 kPa, respectively, outside of nucleus.

is intriguing that concave structural elements in the cell surface are better observed after fixation by glutaraldehyde. However, elasticity measurements have usually been performed in non-fixed cells, because Young's modulus increases dramatically as a consequence of the fixation process.

To investigate cytoskeleton changes induced by PDT at higher resolution we used the AFM topography and force measurement. The height of intact cells was flattened by actin filaments and the nucleus, resulting in a decrease in the height of a normal cell (Sugitate et al. 2009) as can be seen in Figures 2 and 3. Surface mechanical properties of a cell are mainly defined by the actin cytoskeleton. Furthermore, the structures of organelles are very complicated and these will affect the mechanical properties of the cell. Cellular stiffness might be caused by a combination of several contributing factors. In particular, it can be due to the changes in permeability of the cell membrane, due to the disruption of focal adhesions, i.e. sites where the cytoskeleton connects to the cellular membrane, or finally, due to a partial loss of the actin-filament network (Vilenoet al. 2004). PDT did not significantly change the levels of the main cytoskeleton proteins actin and tubulin, but influenced proteins participating in remodeling of actin and microtubule cytoskeletons. The level of dystrophin that forms the scaffold for

binding the actin cytoskeleton to the plasma membrane and calponin involved in the remodeling of the actin cytoskeleton in growth cones. The level of vinculin that links actin bundles to integrin in focal contacts is decreased (Uzdensky et al. 2012). After oxidative stress, neither actin filaments structure nor microtubularcytoskeleton were significantly modified in HeLa cells (Pletjushkina et al. 2006). On the contrary, Liu et al. observed reorganization of the microfilament and microtubule cytoskeleton during the execution phase of apoptosis after PDT, if phthalocyanine was used like photosensitizer. Cleavage of α -tubulin, cytokeratin 18, and actin by caspases during apoptosis has also been reported (Liu et al. 2010).

In addition, it was observed that a lower concentration of microtubules leads to higher Young's modulus, i.e., to higher cell stiffness (Hagaet al. 2000). A rate of breaking of ten microtubules was determined on 5.6 s after oxidative stress was caused by 0.44 M H_2O_2 using a 50 W mercury lamp (Guo et al. 2006).

In fact, the cell nucleus plays an important role as a central support for maintaining the cell body and as an anchor for cell motility (Sugitate et al. 2009) and it also plays a significant role in the response of cells to mechanical stress. The nucleus skeleton (the nuclear lamina) mainly determines the shape, size, and mechanical properties of the

nucleus, and provides the connection of the nuclear inner membrane to chromatin. The nuclear lamina is a network of lamin polymers and lamin-binding proteins (Starodubtseva 2011). The part of the cell adjacent to the nucleus which shows the highest concentration of microtubules also displays a lower Young's modulus, which indicates that microtubules themselves have no large effect on the measured stiffness. However, if only actin filaments contribute to the cell elasticity, the nucleus area should be as stiff as the surroundings, since stress fibers and the cell cortex extend all over beneath the cellular surface. The distribution of intermediate filaments seems to correspond to the cell elasticity. Intermediate filament (vimentin) is presumably another candidate for the cell elasticity. Both actin filaments and other cytoskeleton filaments such as intermediate filaments should be taken into account to explain the cell elasticity (Starodubtseva 2011).

While the AFM probe contacts the cell at designated points, it is not known if the underlying structure of the cell consists of the cytoskeleton, organelles, or vacuoles, to name a few. Each of these substructures affects the elasticity measurements differently (Mustata et al. 2010). Normal cells have a Young's modulus of about one order of magnitude higher than cancerous ones. The change in elastic proper-

ties might be attributed to a difference in the organization of the cell cytoskeleton. This change is associated with the increased cross-linking of extracellular matrix proteins (Kuznetsova et al. 2007).

Our results revealed that the median and quartile²⁵, quartile⁷⁵ of Young's modulus of the cell surface in the nucleus area of the cancer cell line HeLa was 35.283, 28.061 and 50.416 kPa, respectively, and 107.442, 97.185 and 125.270 kPa, respectively, outside of nucleus. After photodynamic treatment, the median and quartile²⁵, quartile⁷⁵ of Young's modulus of the photodynamically damaged cell surfaces in nucleus area were changed to 61.144, 50.814 and 88.866 kPa, respectively, and to 193.605, 174.196 and 217.614 kPa, respectively, outside of nucleus (Figure 4 and 5). Change after PDT showed a significant shift to the higher values of Young's modulus: more than 73% within the nucleus area, and 80% outside of nucleus area. Measurement was carried out on approximately sixty cells included three independent experiments in each group. The probe was focused on the nuclear area or outside of the nucleus area of the HeLa cells, because lysosomes (where CIAIPcS₂ is preferentially loaded) are situated near the nucleus, preferentially at one pole of the HeLa cells (Panzarini et al. 2006). Determining the cell stiffness around the nucleus is important, because

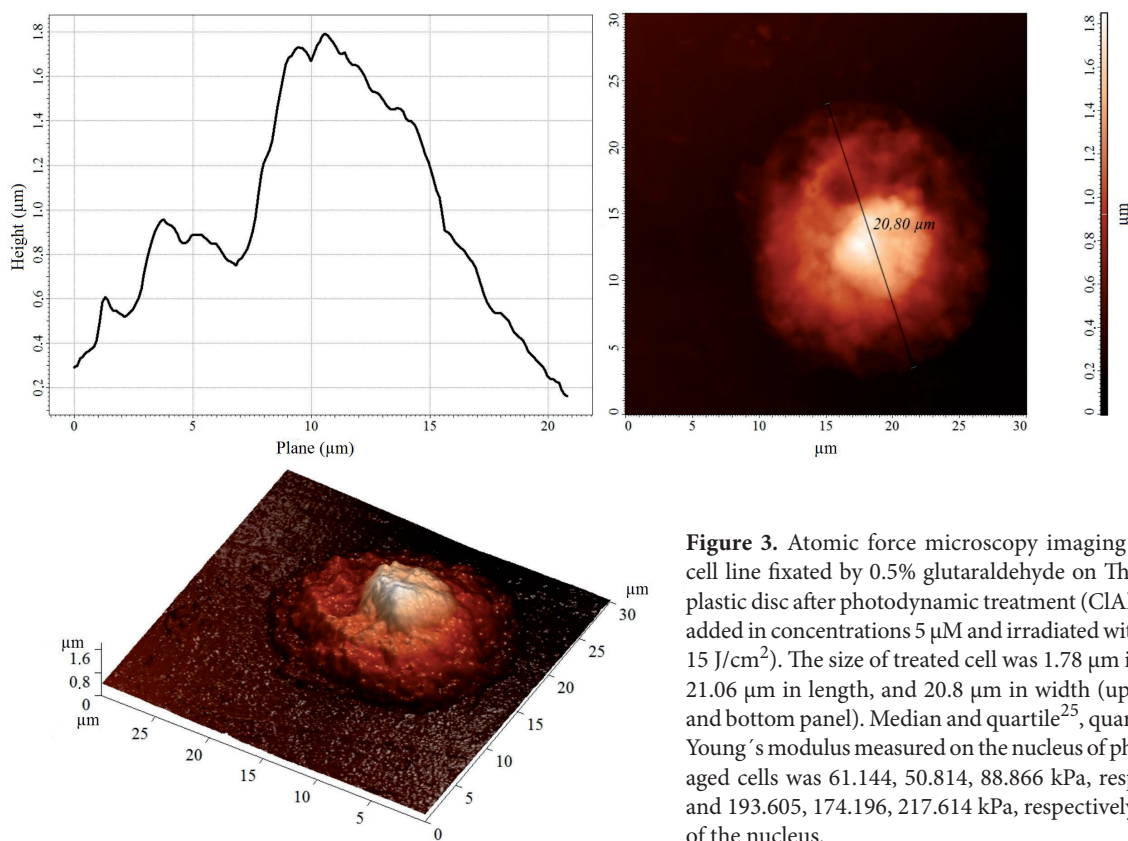


Figure 3. Atomic force microscopy imaging of HeLa cell line fixated by 0.5% glutaraldehyde on Thermanox plastic disc after photodynamic treatment (CIAIPcS₂ was added in concentrations 5 μM and irradiated with dose of 15 J/cm²). The size of treated cell was 1.78 μm in height, 21.06 μm in length, and 20.8 μm in width (upper right and bottom panel). Median and quartile²⁵, quartile⁷⁵ the Young's modulus measured on the nucleus of photodamaged cells was 61.144, 50.814, 88.866 kPa, respectively, and 193.605, 174.196, 217.614 kPa, respectively, outside of the nucleus.

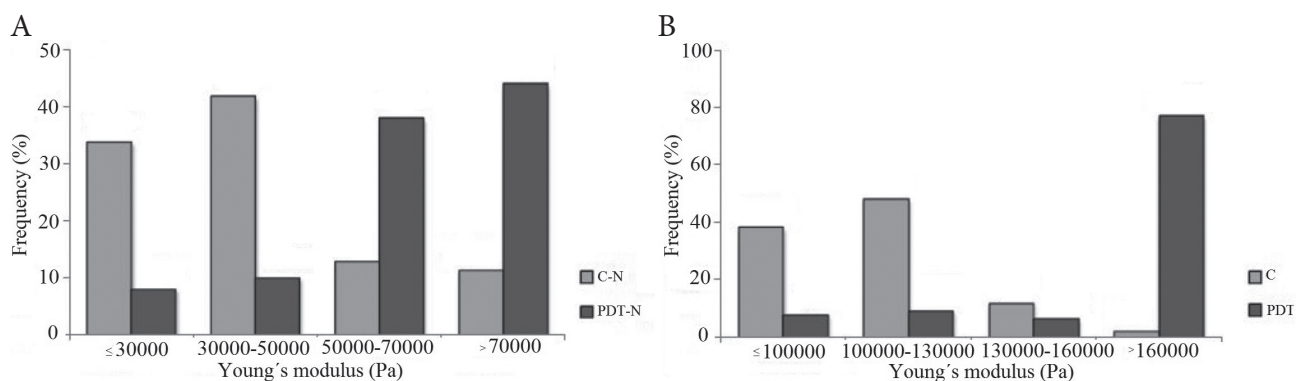


Figure 4. Histograms of frequency of Young's modulus (Pa). Shift of the Young's modulus to the higher values after PDT is significant in a both measured area (nucleus and outside of nucleus) with $p < 0.0001$. C-N, control sample – curves measured on the nucleus; PDT-N, irradiated sample – curves measured on the nucleus (A); C, control sample – curves measured outside the nucleus; PDT, irradiated sample – curves measured outside the nucleus (B).

the relocation of photosensitizers from the lysosomes of treated cells to the cytoplasm and to the nucleus during PDT were observed (Alvarez et al. 2011). Photodamage of lysosomes, as a result of sub-cellular accumulation of photosensitizers, may lead to an increase in lysosomal membrane permeability. Subsequent release of lysosomal enzymes into the cytoplasm would be consistent with the observed and rapid degradation of cytoskeletal proteins and followed by

apoptosis (Liu et al. 2010). Interestingly, this redistribution only occurs after a period of illumination, so it should be considered as a photoinduced relocation due to the release of photosensitizers from their initial organelle targets following photodamage (Alvarez et al. 2011).

The nucleus area is about 10 times softer than the surroundings (Haga et al. 2000). Substrate contributions to the Young's modulus can be neglected if the AFM tip never

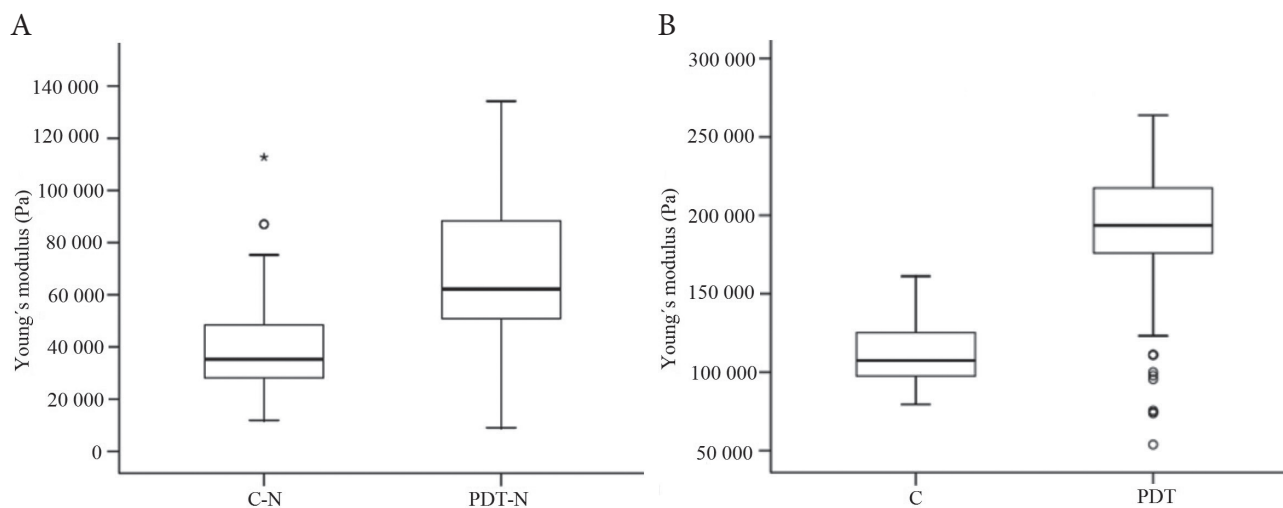


Figure 5. Quartile box graphs describe the distribution of the measured parameter values with quartiles. The thick line inside the box represents the median value (i.e. the second quartile), the bottom of the box represents the first quartile and the top of the box represents the third quartile. Box height corresponds inter-quartile range (i.e. characteristic variability of data – in the interval between the 1st and 3rd quartile is 50% of measured values). Error bars at the bottom and top represent minimum and maximum closed values. Outliers are marked with a ring and star symbol of extreme values. The Mann-Whitney U-test showed significantly higher values in the PDT-N and PDT groups in comparison with the C-N and C group, $p < 0.0001$. C-N, control sample – curves measured on the nucleus; PDT-N, irradiated sample – curves measured on the nucleus (A); C, control sample – curves measured outside the nucleus, PDT, irradiated sample – curves measured outside the nucleus (B).

indented more than 10% of the cell thickness. These results correspond with the measurement of Sugitate et al. in which the surface of hMSCs cell was found to be 54.3 ± 37.37 kPa (Sugitate et al. 2009), with Haga et al. (4–100 kPa) over the cell surface (Haga et al. 2000) and Docheva et al. where Young's modulus of non- and differentiated hMSCs cells was in the range 33–53 kPa (Docheva et al. 2008). It is clear that the estimated values of cell mechanical parameters depend on the experimental methods, on the used theoretical models, dependence on cell type, cell state, and experimental conditions (Starodubsteva 2011). The elasticity of the cell body remained consistent for 1 h and then began to decrease, indicating a loss of rigidity in the cellular cytoskeleton which supports the cellular membrane. This decrease in elasticity continued until a sharp increase toward the Young's modulus of 10 MPa. The measurement of elasticity is not possible if the cell is not securely attached to the sample substrate. Over time, many cells are released from the surface and/or attach to the AFM tip, in addition to degradation which would allow the tip to interact with the surface, thus affecting the elasticity measurements. For this reason, we measured for only a half an hour outside the incubator.

The changes in mechanical properties and cytoskeleton reorganization can be correlated with cell cycle stages, and the results form the basis for understanding the mechanisms of cell differentiation, organism aging (Starodubsteva 2011) or cell death. The stiffness distribution of cell surface can be quite constant for stationary cells, but if the cells start to move, the stiffness in their nuclear regions can be drastically decreased (Kuznetsova et al. 2007). The important factor is the heterogeneity of mechanical properties of cells within different cell regions. In the literature, PDT effect has not been studied in terms of cytomechanical properties of tumor cell lines. For this reason it is not yet possible to determine the data as accurate for clinical use and this can be considered a pilot study of this issue.

Conclusion

It is now well accepted that cell functions are essentially determined by their structure. At different hierarchical levels, the structural organization of cells is characterized by certain mechanical properties. AFM probing of whole cells is an effective tool for studying membrane and sub-membrane cell structures. As the heterogeneity of cell mechanical properties is mainly defined by the membrane cytoskeleton, AFM probing of the cell elasticity can be effectively used in the investigation of cytoskeleton characteristics and dynamics, for example, after photodynamic damage. Our results show changes in cytomechanical properties after photodynamic treatment of more than 70% and 80%. Studies focusing on biomechanics and the biophysical properties of cells are

important in the understanding of the onset and progression of disease states and treatments of cancer at the cellular level. Our study demonstrates the importance using of relatively novel microscopy techniques in understanding mechanical regulation by crucial cellular processes, such as cell death caused by PDT.

Acknowledgements. This work was supported by the Ministry of Education of the Czech Republic KONTAKT LH12085 and CZ.1.05/2.1.00/01.0030.

References

- Alvarez M., Villanueva A., Acedo P., Canete M., Stockert J. C. (2011): Cell death causes relocalization of photosensitizing fluorescent probes. *Acta Biochem.* **113**, 363–368
- Casas A., Sanz-Rodríguez F., Di Venosa G., Rodríguez L., Mamone L., Blázquez A., Jaén P., Batlle A., Stockert J. C., Juarranz A. (2008): Disorganisation of cytoskeleton in cells resistant to photodynamic treatment with decreased metastatic phenotype. *Cancer Lett.* **270**, 56–65
<http://dx.doi.org/10.1016/j.canlet.2008.04.029>
- Casuso I., Rico F., Scheuring S. (2011): Biological AFM: where we come from – where we are – where we may go. *J. Mol. Recognit.* **24**, 406–413
<http://dx.doi.org/10.1002/jmr.1081>
- Docheva D., Padula D., Popov C., Mutschler W., Clausen-Schaumann H., Schieker M. (2008): Researching into the cellular shape, volume and elasticity of mesenchymal stem cells, osteoblasts and osteosarcoma cells by atomic force microscopy. *J. Cell. Mol. Med.* **12**, 537–552
<http://dx.doi.org/10.1111/j.1582-4934.2007.00138.x>
- Fernández-Guarino M., García-Morales I., Harto A., Montull C., Pérez-García B., Jaén P. (2007): Photodynamic therapy: new indications. *Actas Dermo-Sifiliográficas (English Edition)* **98**, 377–395
[http://dx.doi.org/10.1016/S0001-7310\(07\)70091-1](http://dx.doi.org/10.1016/S0001-7310(07)70091-1)
- Guo H., Xu C., Liu C., Qu E., Yuan M., Li Z., Cheng B., Zhang D. (2006): Mechanism and dynamics of breakage of fluorescent microtubules. *Biophys. J.* **90**, 2093–2098
<http://dx.doi.org/10.1529/biophysj.105.071209>
- Haga H., Sasaki S., Kawabata K., Ito E., Ushiki T., Sambongi T. (2000): Elasticity mapping of living fibroblasts by AFM and immunofluorescence observation of the cytoskeleton. *Ultra-microscopy* **82**, 253–258
[http://dx.doi.org/10.1016/S0304-3991\(99\)00157-6](http://dx.doi.org/10.1016/S0304-3991(99)00157-6)
- Jung S. H., Park J. Y., Yoo J. O., Shin I., Kim Y. M., Ha Q. S. (2009): Identification and ultrastructural imaging of photodynamic therapy - induced microfilaments by atomic force microscopy. *Ultramicroscopy* **109**, 1428–1434
<http://dx.doi.org/10.1016/j.ultramic.2009.07.009>
- Ketene A. N., Schmelz E. M., Roberts P. C., Agah M. (2012): The effects of cancer progression on the viscoelasticity of ovarian cell cytoskeleton structures. *Nanomedicine* **8**, 93–102
<http://dx.doi.org/10.1016/j.nano.2011.05.012>
- Kolarova H., Nevrelouva P., Tomankova K., Kolar P., Bajgar R., Mosinger J. (2008): Production of reactive oxygen species after

- photodynamic therapy by porphyrinsensitizers. *Gen. Physiol. Biophys.* **27**, 101–105
- Kuznetsova T. G., Starodubtseva M. N., Yegorenkov N. I., Chizhik S. A., Zhdanov R. I. (2007): Atomic force microscopy probing of cell elasticity. *Micron* **38**, 824–833
<http://dx.doi.org/10.1016/j.micron.2007.06.011>
- Leporatti S., Vergara D., Zacheo A., Vergaro V., Maruccio G., Cingolani R., Rinaldi R. (2009): Cytomechanical and topological investigation of MCF-7 cells by scanning force microscopy. *Nanotechnology* **20**, 055103
<http://dx.doi.org/10.1088/0957-4484/20/5/055103>
- Li Q. S., Lee G. Y. H., Ong C. N., Lim C. T. (2008): AFM indentation study of breast cancer cells. *Biochem. Biophys. Res. Commun.* **374**, 609–613
<http://dx.doi.org/10.1016/j.bbrc.2008.07.078>
- Liu T., Wua L. Y., Berkman C. E. (2010): Prostate-specific membrane antigen-targeted photodynamic therapy induces rapid cytoskeletal disruption. *Cancer Lett.* **296**, 106–112
<http://dx.doi.org/10.1016/j.canlet.2010.04.003>
- Malham G. M., Thomsen R. J., Finlay G. J., Baguley B. C. (1996): Subcellular distribution and photocytotoxicity of aluminiumphthalocyanines and haematoporphyrin derivative in cultured human meningioma cells. *Br. J. Neurosurg.* **10**, 51–57
<http://dx.doi.org/10.1080/02688699650040520>
- Moreno-Flores S., Benitez R., DmVivanco M., Toca-Herrera J. L. (2010): Stress relaxation and creep on living cells with the atomic force microscope: a means to calculate elastic moduli and viscosities of cell components. *Nanotechnology* **21**, 445101
<http://dx.doi.org/10.1088/0957-4484/21/44/445101>
- Muller D. J., Dufrêne Y. F. (2011): Atomic force microscopy: a nanoscopic window on the cell surface. *Trends Cell Biol.* **21**, 461–469
<http://dx.doi.org/10.1016/j.tcb.2011.04.008>
- Mustata N., Ritchie K., McNally H. A. (2010): Neuronal elasticity as measured by atomic force microscopy. *J. Neurosci. Meth.* **186**, 35–41
<http://dx.doi.org/10.1016/j.jneumeth.2009.10.021>
- Nikkhah M., Strobl J. S., De Vita R., Agah M. (2010): The cytoskeletal organization of breast carcinoma and fibroblast cells inside three dimensional (3-D) isotropic silicon microstructures. *Biomaterials* **31**, 4552–4561
<http://dx.doi.org/10.1016/j.biomaterials.2010.02.034>
- Panzarini E., Tenuzzo B., Palazzo F., Chionna A., Dini L. (2006): Apoptosis induction and mitochondria alteration in human HeLa tumour cells by photoproducts of Rose Bengal acetate. *J. Photochem. Photobiol. B: Biology* **83**, 39–47
<http://dx.doi.org/10.1016/j.jphotobiol.2005.11.014>
- Pletjushkina O. Y., Lyamzaev K. G., Popova E. N., Nepryakhina O. K., Ivanova O. Y., Domnina L. V., Chernyak B. V., Skulachev V. P. (2006): Effect of oxidative stress on dynamic of mitochondrial reticulum. *Biochim. Biophys. Acta* **1757**, 518–524
<http://dx.doi.org/10.1016/j.bbabo.2006.03.018>
- Pluskalová M., Peslova G., Grebenova D., Halada P., Hrkal Z. (2006): Photodynamic treatment (ALA-PDT) suppresses the expression of the oncogenic Bcr-Abl kinase and affects the cytoskeleton organization in K562 cells. *J. Photochem. Photobiol. B-Biol.* **83**, 205–212
- Riethmuller C., Schaffer T. E., Kienberger F., Stracke W., Oberleithner H. (2007): Vacuolar structures can be identified by AFM elasticity mapping. *Ultramicroscopy* **107**, 895–901
<http://dx.doi.org/10.1016/j.ultramic.2007.04.007>
- Sader J. E., Chon J. W. M., Mulvaney P. (1999): Calibration of rectangular atomic force microscope cantilevers. *Rev. Scientific Instr.* **70**, 3967–3969
<http://dx.doi.org/10.1063/1.1150021>
- Sanabria L. M., Rodriguez M. E., Cogno I. S., Vittar N. B. R., Pansa M. F., Lamberti M. J., Rivarola V. A. (2013): Direct and indirect photodynamic therapy effects on the cellular and molecular components of the tumor microenvironment. *Biochim. Biophys. Acta-Rev. Cancer* **1835**, 36–45
- Sugitate T., Kihara T., Liu X. Y., Miyake J. (2009): Mechanical role of the nucleus in a cell in terms of elastic modulus. *Curr. Appl. Phys.* **9**, e291–293
<http://dx.doi.org/10.1016/j.cap.2009.06.020>
- Sullivan C. J., Venkataraman S., Retter S. T., Allison D. P., Doktycz M. J. (2007): Comparison of the indentation and elasticity of *E. coli* and its spheroplasts by AFM. *Ultramicroscopy* **107**, 934–942
<http://dx.doi.org/10.1016/j.ultramic.2007.04.017>
- Suresh S. (2007): Biomechanics and biophysics of cancer cells. *Acta Biomaterialia* **3**, 413–438
<http://dx.doi.org/10.1016/j.actbio.2007.04.002>
- Sneddon I. N. (1965): The relaxation between load and penetration in the axisymmetric Boussinesq problem for a punch of arbitrary profile. *Int. J. Engng. Sci.* **3**, 47–57
[http://dx.doi.org/10.1016/0020-7225\(65\)90019-4](http://dx.doi.org/10.1016/0020-7225(65)90019-4)
- Starodubtseva M. N. (2011): Mechanical properties of cell and aging. *Ageing Res. Rev.* **10**, 16–25
<http://dx.doi.org/10.1016/j.arr.2009.10.005>
- Tomankova K., Kolarova H., Vujtek M., Bajgar R. (2007): Photodynamic effect on melanoma cells investigated by atomic force microscopy. *Gen. Physiol. Biophys.* **26**, 200–206
- Uzdensky A., Kolpakova E., Juzeniene A., Juzenas P., Moana J. (2005): The effect of sub-lethal ALA-PDT on the cytoskeleton and adhesion of cultured human cancer cells. *Biochim. Biophys. Acta* **1722**, 43–50
<http://dx.doi.org/10.1016/j.bbagen.2004.11.011>
- Uzdensky A., Kristiansen B., Moan J., Juzenien A. (2012): Dynamics of signaling, cytoskeleton and cell cycle regulation proteins in glioblastoma cells after sub-lethal photodynamic treatment: Antibody microarray study. *Biochim. Biophys. Acta* **1820**, 795–803
<http://dx.doi.org/10.1016/j.bbagen.2012.03.008>
- Vegh A. G., Fazakas C., Nagy K., Wilhelm I., Molnar J., Krizbai I. A., Szegletes Z., Varo G. (2012): Adhesion and stress relaxation forces between melanoma and cerebral endothelial cells. *Eur. Biophys. J.* **41**, 139–145
<http://dx.doi.org/10.1007/s00249-011-0765-5>
- Vileno B., Sienkiewicz A., Lekka M., Kulik A. J., Forro L. (2004): In vitro assay of singlet oxygen generation in the presence of water-soluble derivatives of C60. *Carbon* **42**, 1195–1198
<http://dx.doi.org/10.1016/j.carbon.2003.12.042>

Received: August 29, 2012

Final version accepted: February 25, 2013